

Exact coherent structures and their instabilities: toward a dynamical-system theory of shear turbulence¹

Fabian Waleffe

*Departments of Mathematics and Engineering Physics
University of Wisconsin-Madison, USA*

Exact coherent structures are steady state or traveling wave solutions of the Navier-Stokes equations that bifurcate from a neutrally stable streaky flow. Such solutions exist in various shear flows, for example in free-slip and no-slip plane Couette and Poiseuille flows, and are homotopic to one another. They are smoothly connected to each other through simple mappings in parameter space and their forms in physical space are also closely related. These non-turbulent solutions capture the main structural and statistical features of turbulent flows, such as the form and characteristic sizes of the coherent structures, yet they are unstable from onset. A simple 1D discrete dynamical system illustrates how unstable solutions can be relevant to the dynamics and are symptomatic of a ‘hard’ transition to turbulence. Fully-resolved steady states in no-slip plane Couette flow are presented for various length scales up to Reynolds number 400 where turbulent and time-periodic solutions have been obtained.

1 Introduction

The question of whether shear turbulence can be understood from the point of view of dynamical systems has been discussed many times since the discoveries of the period doubling and other routes to Chaos in low-order systems. It has been argued that ‘open’ systems such as shear turbulence are fundamentally different from ‘closed’ systems such as Rayleigh-Bénard convection. A distinction has been drawn between *absolute* and *convective* instabilities and experiments suggest that the onset of shear turbulence is a complex spatio-temporal process characterized by the development of *turbulent spots*.

Nonetheless, I believe that a dynamical-systems understanding of the onset of shear turbulence is forthcoming and intimately tied with the near-wall coherent structures that have been studied experimentally for about 50 years. The impact of coherent structures on our views of the statistical nature of turbulence and turbulent transport has been profound but largely

¹©by Fabian Waleffe, September 25, 2002. Reproduced with permission for the Proceedings of the International Symposium on “Dynamics and Statistics of Coherent Structures in Turbulence: Roles of Elementary Vortices”, Tokyo, Japan, October 21-23, 2002.

qualitative because of a lack of an adequate quantitative mathematical model of the coherent structures. Precise mathematical models of the coherent structures are now available in the form of steady state and traveling wave solutions of the Navier-Stokes equations. These *exact coherent structures* are unstable from onset typically. Therefore, this suggests a precise definition of Townsend’s notions of ‘active’ and ‘inactive’ motions as the exact coherent structures and their instabilities, respectively. The study of the exact coherent structures, their instabilities and subsequent bifurcations is expected to lead to an understanding of the onset and nature of shear turbulence and of the issues of ‘bursting’ and streak spacing. In a second stage, studies of the self-organization of the coherent structures in large spatial domains and of their interaction with the laminar flow should lead to an elucidation of complex spatio-temporal processes such as spots at transitional Reynolds numbers and packets of horseshoe vortices in fully developed turbulence at moderate Reynolds numbers, studied recently by Adrian and co-workers [1]. The difficulty in understanding shear turbulence is seen not as a result of the difference between absolute and convective instabilities, but as a result of the linear stability of the laminar flow, essentially for all Reynolds numbers, and the importance of unstable three-dimensional nonlinear states that appear ‘out-of-the-blue-sky’ at Reynolds numbers of a few hundreds.

This union of dynamical-systems theory with coherent structures has been pursued by others, most notably by Holmes, Lumley and their co-workers [5]. However, their approach has been aimed at modeling developed turbulence and is based on a projection of the Navier-Stokes equations on empirical orthogonal functions (EOF, also known as POD modes) that incorporate dynamical features reflected in the turbulence statistics, such as the self-sustenance of quasi-streamwise vortices and streaks, through spurious kinematic constraints [15]. Our approach is aimed first at elucidating the onset of turbulence for the fully resolved Navier-Stokes equations. Low-order models faithful to the Navier-Stokes dynamics are used for illustrative purposes only at this stage. In particular, a 4th order model provides a simple mathematical model of the fundamental dynamical process by which quasi-streamwise vortices and streaks sustain each other in a shear flow. The model leads to useful insights that apply to fully resolved solutions of the Navier-Stokes equations as shown below (see [3] for comparison of the model with experimental observations).

The underlying physical mechanisms and the methods used to compute the exact coherent structures in plane Couette and Poiseuille flows are briefly reviewed below. The focus here is on the steady state solutions in plane Couette flow, first calculated by Nagata [11], and on drawing connections between the steady states, the time periodic solution discovered by Kawahara and Kida [9] and turbulent flows.

2 Mathematical and numerical formulation

The mathematical setting of the problem consists of the Navier-Stokes equations for the evolution of the divergence-free velocity field $\mathbf{v}(\mathbf{x}, t)$

$$\begin{aligned} \frac{\partial \mathbf{v}}{\partial t} + \mathbf{v} \cdot \nabla \mathbf{v} &= -\nabla p + \frac{1}{R} \nabla^2 \mathbf{v} + \mathbf{F}, \\ \nabla \cdot \mathbf{v} &= 0, \end{aligned} \tag{1}$$

where p is the kinematic pressure and R the Reynolds number. \mathbf{F} is an external driving force such as the imposed pressure gradient in plane Poiseuille flow. The flow domain is a channel

bounded by two parallel rigid walls at $y = \pm 1$ with periodic boundary conditions imposed in the streamwise x and spanwise z directions, with periodicity $2\pi/\alpha$ and $2\pi/\gamma$, respectively. Pressure is eliminated by the ‘roll-streak’ projection of the equations $-\hat{\mathbf{y}} \cdot \nabla \times (\nabla \times (\cdot))$ and $\hat{\mathbf{y}} \cdot \nabla \times (\cdot)$ and the divergence-free flow is completely described in terms of the three-dimensional y components of velocity $v(\mathbf{x}, t)$ and vorticity $\eta(\mathbf{x}, t)$ together with the one-dimensional mean flow $\bar{U}(y, t)$. Numerically, these fields are expanded in terms of Fourier modes in x and z and integrals of Chebyshev polynomials that satisfy the boundary conditions in y :

$$v = \sum_{l=-L_T}^{L_T} \sum_{m=0}^{M_T} \sum_{n=-N_T}^{N_T} A_{lmn} e^{il\alpha x} e^{in\gamma z} \phi_m(y), \quad (2)$$

$$\eta = \sum_{l=-L_T}^{L_T} \sum_{m=0}^{M_T} \sum_{n=-N_T}^{N_T} B_{lmn} e^{il\alpha x} e^{in\gamma z} \psi_m(y), \quad (3)$$

$$\bar{U} = U_b(y) + \sum_{m=0}^{M_T} \hat{u}_m \psi_m(y). \quad (4)$$

where $D^4 \phi_m(y) = T_m(y)$, $D^2 \psi_m(y) = T_m(y) - \bar{T}_m$ with $\bar{T}_m = (1/2) \int_{-1}^1 T_m(y) dy$ and $U_b(y)$ is the laminar base flow. An elliptical cutoff that truncates modes with

$$\frac{l^2}{(L_T + 1)^2} + \frac{m^2}{(M_T + 1)^2} + \frac{n^2}{(N_T + 1)^2} \geq 1 \quad (5)$$

is used to reduce the problem to a finite size. This resolution approximately corresponds to a direct numerical simulation with resolution $(2L_T + 1) \times (M_T + 5) \times (2N_T + 1)$ after de-aliasing in x and z . Steady states and traveling wave solutions of the truncated Navier-Stokes equations are calculated using Newton’s method together with continuation and homotopy procedures. Further discussions of the mathematics and numerics are given in [18].

3 Bifurcation from streaky flow and homotopy

The physical mechanisms underlying the coherent structures have been described as a three-dimensional self-sustaining process in which streamwise rolls redistribute the mean streamwise velocity to sustain streaks whose inflectional instability nonlinearly sustains the rolls [14, 15]. That process, whose main ingredients consist of the one-dimensional mean shear, two-dimensional x -independent rolls and streaks (kinematically distinct from the rolls) and a three-dimensional streak instability eigenmode, has been described in simple terms by the fourth-order model

$$\begin{pmatrix} \left(\frac{d}{dt} + \kappa_m^2/Re\right) M = & \kappa_m^2/R & -\sigma_u UV & & +\sigma_m W^2 \\ \left(\frac{d}{dt} + \kappa_u^2/Re\right) U = & & \sigma_u MV & -\sigma_w W^2 & \\ \left(\frac{d}{dt} + \kappa_v^2/Re\right) V = & & & \sigma_v W^2 & \\ \left(\frac{d}{dt} + \kappa_w^2/Re\right) W = & & \sigma_w UW & -\sigma_v VW & -\sigma_m MW \end{pmatrix} \quad (6)$$

where the κ 's and σ 's are positive real constants and $M(t)$, $U(t)$, $V(t)$ and $W(t)$ represent the real amplitudes of the mean shear, the streaks, the rolls and the streak eigenmodes, respectively. The nonlinear terms on the right-hand side are quadratic and energy conserving. They are organized in columns to show the self-sustaining process and energy conservation. The mean shear is forced externally by the constant term κ_m^2/R ; the streaks U originate from the redistribution of mean shear M by the rolls V ; the streaks U are linearly unstable to W ; finally, the nonlinear self-interaction of W forces V . The last column represents a feedback of the streak eigenmode W onto the mean shear M . This is not needed for the self-sustaining process but exists in general, as shown by the Galerkin derivation from the Navier-Stokes equations in [15]. Note that that term provides a nonlinear stabilization of the laminar flow.

These equations have a simple laminar fixed point $(M, U, V, W) = (1, 0, 0, 0)$ which is *stable for all Reynolds numbers*. But there are also non-trivial fixed points, typically unstable from onset, that exists above a certain finite Reynolds number. Homoclinic bifurcations to periodic solutions have also been observed (see [14, 15] for details) but it is noteworthy that chaotic solutions have not been seen. This simple 4th order characterization of the self-sustaining process suggests that the self-sustaining process could lead to non-trivial steady states (or traveling waves) as well as time-periodic states in the full Navier-Stokes equations. Indeed, the work of Kawahara and Kida reveals the existence of time-periodic solutions, first suggested by the work of Hamilton *et al.* [6], that are fully consistent with the self-sustaining process. In addition, we have demonstrated that the steady states can be calculated by continuation of three-dimensional solutions that bifurcate from two-dimensional streaky flows thereby establishing a direct link between the streaky flow instability, the self-sustaining process and three-dimensional self-sustained solutions of the Navier-Stokes equations that consist of wavy streaks flanked with staggered quasi-streamwise vortices.

That procedure was carried out in [16, 18] for the full Navier-Stokes equations, but will be illustrated here in simple terms using the 4th order model. The procedure consists in tracking solutions that bifurcate from an unstable, two-dimensional streaky flow. To do so, a small $O(1/R^2)$ external forcing is added to the right of the streamwise rolls V -equation which then reads

$$\left(\frac{d}{dt} + \frac{\kappa_v^2}{R}\right) V = \frac{\kappa_v^2 F}{R^2} + \sigma_v W^2 \quad (7)$$

where F is a positive parameter. The laminar state then becomes the (2D) streaky flow

$$(M, U, V, W) = (M_0, U_0, V_0, 0) \equiv \left(\frac{\kappa_m^2 \kappa_u^2}{\kappa_m^2 \kappa_u^2 + \sigma_u^2 F^2}, \frac{\sigma_u \kappa_m^2 F}{\kappa_m^2 \kappa_u^2 + \sigma_u^2 F^2}, \frac{F}{R}, 0\right). \quad (8)$$

Clearly $M_0 \leq 1$ and U_0 are $O(1)$ while $V_0 = F/R$ is $O(1/R)$. Inspection of the W equation shows that this streaky flow (8) is unstable if the exponential growth rate of W , λ_w say, is positive:

$$\lambda_w \equiv (\sigma_w U_0 - \sigma_v V_0 - \sigma_m M_0) - \frac{\kappa_w}{R} > 0. \quad (9)$$

Inspection of (8) shows that this is always possible if F and R are sufficiently large. In fact, $\lambda_w = 0$ (neutral stability) occurs at $F \equiv F_0$ with

$$F_0 = \frac{\kappa_u^2 \sigma_m}{\sigma_u \sigma_w} + O(1/R). \quad (10)$$

Therefore, for fixed R sufficiently large, a branch of non-trivial steady states bifurcates from the point $(F, W) = (F_0, 0)$ in the F - W plane. It is clear from eqn. (7) that the W^2 term

can take the place of the weak external roll forcing $\kappa_v F/R^2$ if $W = O(1/R)$. At large R , the W^2 terms can then be neglected in the M and U equations but not in the V equation and approximate non-trivial steady states are $(M, U, V, W) \approx (M_0, U_0, V_0, W)$, with M_0 , U_0 and V_0 as in (8) but with F_0 in place of F for neutral stability, and F and W such that

$$F \approx F_0 - (\sigma_v/\kappa_v^2)R^2W^2. \quad (11)$$

This equation describes the branch of solutions in the neighborhood of $(F_0, 0)$ and indicates that the bifurcation from streaky flow is subcritical, as should be if the process is indeed self-sustaining.

For the low-order model it is easy enough to get the full F - W equation describing the manifold of steady states. Eliminating M , U and V from the equations (6) with $d/dt = 0$ and the V equation replaced by the forced equation (7), the steady states must satisfy the multi-cubic polynomial equation

$$\begin{aligned} & \sigma_v \sigma_u^2 (F^3 + X^3) + \kappa_w^2 \sigma_u^2 (F^2 + X^2) + \kappa_m^2 (\sigma_v \kappa_u^2 - \sigma_w \sigma_u R) (F + X) + \\ & \frac{\kappa_v^2}{\sigma_v} (\sigma_m^2 \kappa_u^2 + \sigma_w^2 \kappa_m^2) X + 2\kappa_w^2 \sigma_u^2 F X + 3\sigma_v \sigma_u^2 F X (F + X) + \sigma_m \kappa_m^2 \kappa_u^2 R + \kappa_w^2 \kappa_m^2 \kappa_u^2 = 0 \end{aligned} \quad (12)$$

where $X = (\sigma_v/\kappa_v^2)R^2W^2$ so $V = (F + X)/R$. Note that this is a slightly different X definition than in [15]. This expression is almost perfectly symmetric in F and X except for two terms linear in X that originate from the nonlinear feedback of the streak undulation W onto the streaks U and the mean M . For large R , the solution is $F + X = (\kappa_u^2 \sigma_m)/(\sigma_u \sigma_w) + O(1/R)$, recovering (10) and (11), but in addition, when $F = 0$, this yields a non-trivial self-sustained steady state with $X = (\kappa_u^2 \sigma_m)/(\sigma_u \sigma_w) + O(1/R)$. More generally, the bifurcation points are given by the solutions $F = F_0$ of (12) with $X = 0$, while the non-trivial self-sustained states are obtained from the solutions of the same equation but with $F = 0$. The analysis of those two cases is identical to that in Sect. III.D. of [15]. One concludes that there is a critical Reynolds number R_1 above which there are two $F_0 > 0$ between which the streaky flow (8) is unstable, and another critical Reynolds number $R_2 > R_1$ above which there are two solutions with $X > 0$ and $F = 0$, corresponding to non-trivial self-sustained steady states. That analysis suggests that (12) consists of a closed curve in the right quadrant of the F - X plane that intercepts the F and X axes if $R > R_2$. There is also a separate branch of solutions of (12) that crosses the F and X axes at negative values of $O(R^{1/2})$ as $R \rightarrow \infty$. That branch is not of interest in this work as $X \geq 0$ and the forcing opposes nonlinear feedback when $F < 0$. In summary, the physically interesting branch of solutions of (12) in the F - W plane has the form shown in fig. 1. Remarkably, these features of the bifurcation from streaky flow and of the self-sustained states in the 4th order model are also observed for the Navier-Stokes equations. Indeed, fig. 1 is actually obtained from the Navier-Stokes equations with resolution $(L_T, M_T, N_T) = (9, 17, 9)$ in the case of plane Couette-flow with imposed stress at the walls. In fig. 1, W is defined as the y -average of the $l = 1, n = 0, \eta$ mode.

This bifurcation from streaky flow procedure can be used to calculate steady states in no-slip plane Couette flow as well as to calculate traveling wave solutions in free-slip and no-slip plane Poiseuille flow. However, the appropriate roll forcing required for Poiseuille flow is trickier to determine as it turns out to be more concentrated in the center of the (half) channel than in plane Couette flow. Once a self-sustained state has been found in one flow, it is simpler to calculate solutions in other flows by homotopy, *i.e.* by smoothly deforming plane Couette

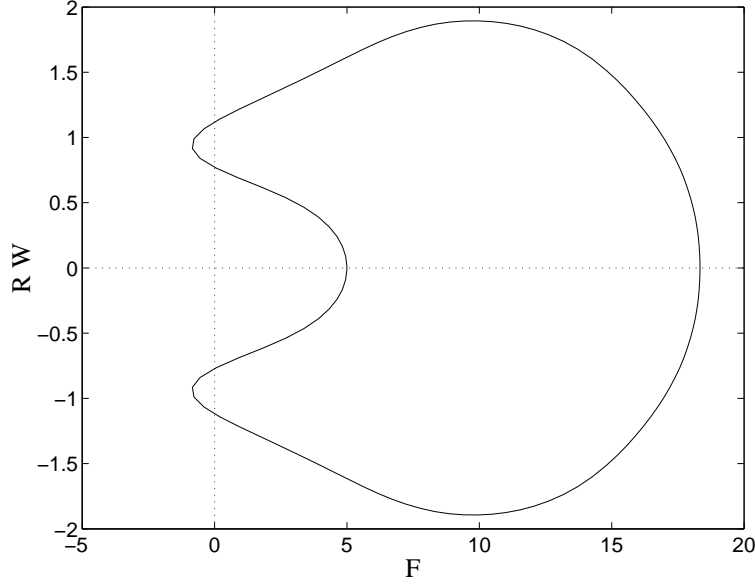


Figure 1: Bifurcation from streaky flow: W (scaled by R) versus roll forcing parameter F corresponding to a steady state solution of the Navier-Stokes equations in free-free plane Couette with $(\alpha, \gamma) = (0.49, 1.5)$ at $R = 150$ with resolution $(L_T, M_T, N_T) = (9, 17, 9)$.

into plane Poiseuille flow. The appropriate homotopy is to map the full channel plane Couette flow into a half-channel plane Poiseuille flow according to the formula

$$U_b(y; \mu) \equiv y + \mu \left(\frac{1}{6} - \frac{y^2}{2} \right). \quad (13)$$

For $\mu = 0$, This is the laminar plane Couette flow when $\mu = 0$ and a half laminar Poiseuille flow when $\mu = 1$. The boundary conditions corresponding to that half-Poiseuille flow consists of no-slip at $y = -1$ and free-slip at $y = 1$. Therefore, homotopies from free-slip to no-slip are also required. Those are performed by use of the boundary conditions

$$\begin{aligned} v &= \lambda_t \partial_y v + \kappa_t \partial_y^2 v = \lambda_t \eta + \kappa_t \partial_y \eta = 0, \\ v &= \lambda_b \partial_y v - \kappa_b \partial_y^2 v = \lambda_b \eta - \kappa_b \partial_y \eta = 0 \end{aligned} \quad (14)$$

at $y = +1$ and $y = -1$, respectively, where $0 \leq \lambda \leq 1$ and $\kappa = 1 - \lambda$. These yield free-slip when $\lambda = 0$ and no-slip when $\lambda = 1$.

These homotopies demonstrate the close relationships between the exact coherent structures in both plane Couette and Poiseuille flows with either free-slip or no-slip. All these solutions are part of the same manifold of solutions.

Once a solution has been found in one flow, it can be continued to other values of the Reynolds numbers and horizontal periodic lengths. Therefore, for a given flow and boundary conditions, the exact coherent structures form a 3D manifold of solutions parametrized by α , γ and R . It is particularly interesting to determine the lowest Reynolds number at which these solutions exist. For no-slip plane Poiseuille flow, this is $R = 244.36$ achieved at $(\alpha, \gamma) = (0.5074, 1.3165)$. That solution has an average velocity with respect to the wall of $\langle U \rangle = 0.886$ and a bulk Reynolds number (based on the full channel width and the average flow velocity)

of $R_m = 866$. In wall units, this corresponds to

$$L_x^+ = 273.73, L_z^+ = 105.51, 2h^+ = 44.21. \quad (15)$$

These values are remarkably close to the typical values observed in the near-wall region of turbulent flows [12]. The lowest Reynolds number for no-slip plane Couette 3D steady states is

$$R_{sn} = 127.7 \quad \text{at} \quad (\alpha, \gamma) = (0.5772, 1.1506). \quad (16)$$

That solution has $\left|d\bar{U}/dy\right|_{wall} = 1.8087$, therefore those values correspond to the wall units values

$$L_x^+ = 165, L_z^+ = 83, 2h^+ = 30. \quad (17)$$

These steady states have been illustrated in [17] and [18]. They consists of wavy streaks flanked by staggered quasi-streamwise vortices. In the following, I focus on further parametric studies of the plane Couette flow steady states, complementing the results already reported in [18].

4 No-slip plane Couette flow steady states

The wavenumbers leading to the lowest Reynolds number for the steady states are $\alpha = 0.5772$ and $\gamma = 1.1506$. The studies of Clever and Busse [4] suggest that the relation $\gamma \approx 2\alpha$ lead to the lowest Reynolds numbers. This is understood in terms of the streak instability in [18]. The streak instability is of inflectional nature. Hence one expects that it requires $\alpha < \gamma$ [14]. The symmetric steady states seem to disappear if α is greater than about $2\gamma/3$ [18] consistent with the streak instability results. Instability to asymmetric traveling waves occurs for larger α (see fig. 6 in [15]).

Hamilton *et al.* [6] focused on the parameters $R = 400$ and $(\alpha, \gamma) = (8/7, 5/3) \approx (1.14, 1.67)$ in their early investigations of the self-sustaining process. Those values were obtained by tracking turbulent flows to smaller and smaller box sizes, in a manner similar to that of Jimenez and Moin [8], and settling on those parameters because they revealed the self-sustaining process relatively cleanly through a nearly periodic time evolution. Kawahara and Kida [9] recently re-investigated plane Couette flow for those same parameter values and discovered numerically true time-periodic solutions. They sought to connect those solutions to the steady states using the shooting method of Toh and Itano [7]. The steady state solution they calculated was not directly connected to the periodic solution that is close to the turbulent flow but it is connected to another weaker periodic solution that has heteroclinic connections with the stronger periodic solution.

Bifurcation diagrams are given here for no-slip plane Couette flow steady states with (α, γ) related to the parameters $(\alpha_0, \gamma_0) \equiv (1.14, 1.67)$ used in [6], [9] in order to complete the bifurcation scenario. Figure 2 (top) shows S , the shear rate at the wall normalized by its laminar value, versus the Reynolds number R for the no-slip plane Couette flow steady states with $\gamma = \gamma_0 \equiv 1.67$ and various α 's. We see that the upper branch steady states collapses rapidly as α is increased above about 1.00 and the solution disappears, in this range of Reynolds numbers, for $\alpha > 1.08$. An 'isola' – a closed branch of solutions – is found for $\alpha = 1.06$. Another isola was found for $\alpha = 1.07$ inside this one (not shown). This abrupt disappearance of the steady states can be understood in terms of the streak instability. In particular, fig. 6 in [15] indicates that the streaks have a single real zero eigenvalue at $R = 400$ only if $\alpha < 1.1$. Therefore, there is no bifurcation of steady states from the streaky flow for $\alpha > 1.1$ at $R = 400$

when $\gamma = 1.67$. That same figure indicates the possibility of bifurcation to asymmetric traveling waves for larger α . In between those two cases is a co-dimension two bifurcation with a double zero eigenvalue. It is possible that this could be a bifurcation point for the periodic solutions.

Figure 2 (bottom) shows S versus R for $\alpha = \alpha_0$ with both $\gamma = 2\alpha_0$, $1.5\gamma_0$ and $2\gamma_0$, demonstrating that steady states solutions reappear at $\alpha = 1.14$ if the spanwise wavenumber γ is increased. Those solutions are pushed to higher Reynolds number in a natural way as γ increases. Note that the normalized wall shear rate S is equal to the normalized energy input rate I used by Kawahara and Kida [9]. Although there is no steady state solution with $(\alpha, \gamma) = (1.14, 1.67)$ at $R = 400$, there are many steady states with related wavenumbers whose upper branches have $S \equiv I$ of the order of that seen for the strong periodic solution of Kawahara and Kida *i.e.* $I \approx 3$, and lower branches with $S \equiv I$ of the order of those seen for the other weaker periodic solution, *i.e.* $I \approx 1.5$.

The structure of one such upper branch solution is illustrated in fig. 3 for $\alpha = \alpha_0$, $\gamma = 1.5\gamma_0$ at $R = 400$ and its mean and RMS velocity profiles are shown in fig. 4. These profiles compare well with the profiles of the turbulent and strong periodic solution in [9]. This does not yet elucidate the bifurcation-theoretic origin of the periodic solutions² but provides a fairly complete picture of related steady states in the α, γ, R parameter space. It seems likely that the strong periodic solution bifurcates from an upper branch steady state but it is also possible, and not contradictory, that the periodic solutions bifurcate directly from the streaky flow at the codimension two point.

5 A simple model of shear turbulence?

The brief review above suggests a connection between upper branch steady states, ‘strong’ time-periodic solutions and turbulent flows. The structure and statistics of the steady states and the periodic solutions certainly suggest connections. However, one might wonder why and how unstable solutions could be dynamically significant and manage to capture structural and statistical features of turbulent flows.

A simple model 1D map is offered here as an illustration of those issues. The model has been discussed in [18] and is the simple discrete dynamical system

$$x_{n+1} = f_\mu(x_n) \equiv \mu \frac{\min(x_n, 1 - x_n)}{\max(x_n, 1 - x_n)} \quad (18)$$

where $0 \leq x_n \leq 1$ and the parameter μ is related to the Reynolds number R as

$$\mu = \frac{R}{R + R_c} \quad (19)$$

for some $R_c > 0$. Clearly $0 \leq \mu < 1$. This model has some analytical similarity with the famous logistic map: $x_{n+1} = 4\mu x_n(1 - x_n)$ but it has a cusp at $x = 1/2$ and is therefore geometrically similar to the Lorenz map. That cusp leads to sudden transition to chaos at $\mu = 1/2$, or $R = R_c$ (see fig. 5).

As discussed in [18], the map has one trivial fixed point $x = 0$ that is stable for all Reynolds numbers. This is the equivalent of the simple stable laminar state in plane Couette flow. As the Reynolds number is increased, there is a bifurcation at $R = R_c$ that introduces two non-trivial

²Their physical origin is no doubt the same self-sustaining process.

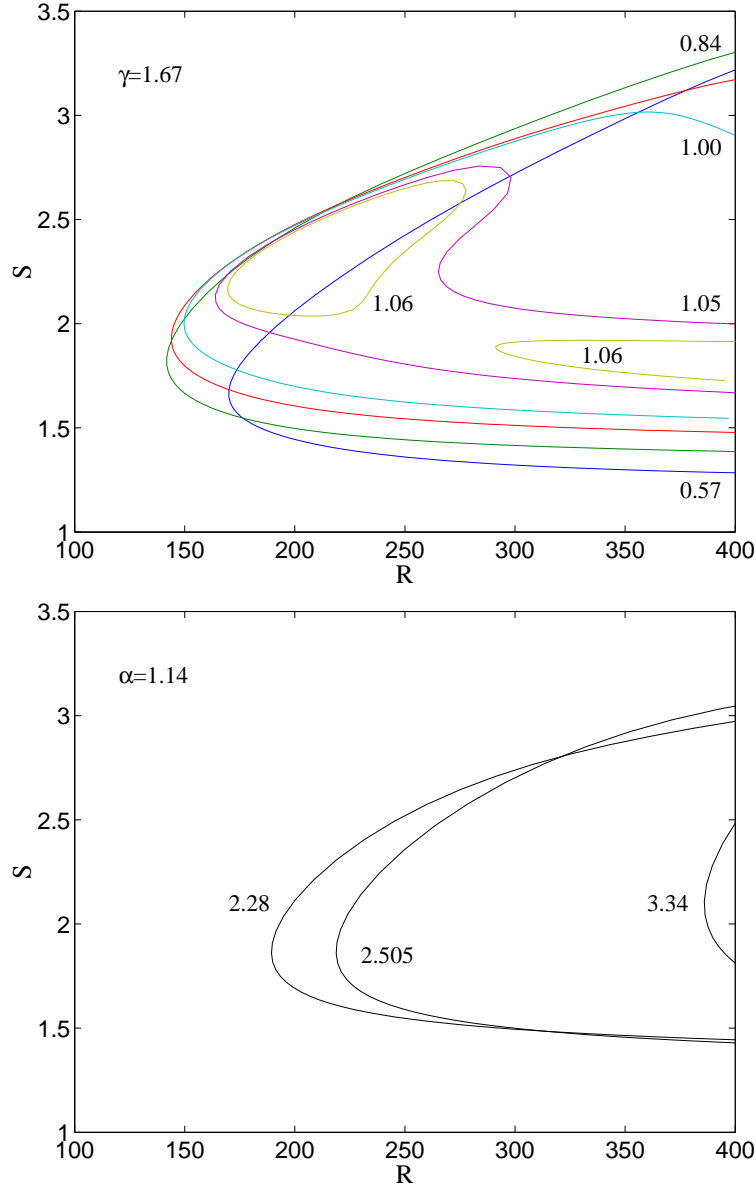


Figure 2: Bifurcation diagrams for steady states in no-slip plane Couette flow. Normalized wall shear rate S versus Reynolds number R . TOP: $\gamma = 1.67$ and $\alpha = 0.57, 0.84, 0.95, 1.00, 1.05$ and 1.06 . At $R = 400$, S increases with α on the lower branch but decreases with α when $\alpha > 0.84$ on the upper branch. BOTTOM: $\alpha = 1.14$ and $\gamma = 2.28, 2.505$ and 3.34 . Various resolutions $(L_T, M_T, N_T) = (13, 25, 13), (13, 27, 13), (15, 27, 15)$, and $(15, 29, 15)$.

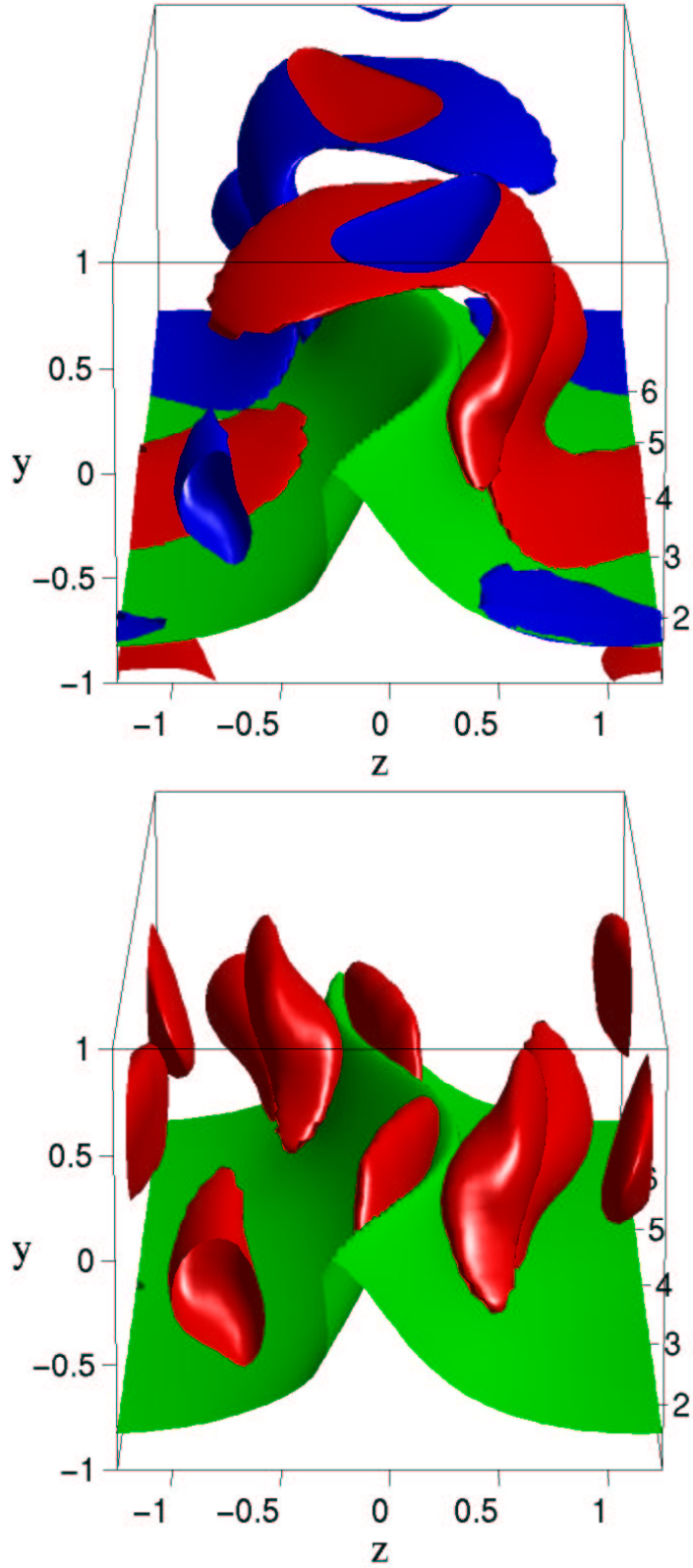


Figure 3: No-slip plane Couette flow steady state: upper branch for $\alpha = 1.14$, $\gamma = 2.505$ at $R = 400$. Top: isosurfaces of streamwise vorticity $\pm(0.6 \max \omega_x) = \pm 0.56$ (red positive, blue negative). Bottom: isosurfaces of $\nabla^2 p = 2Q = W_{ij}W_{ij} - S_{ij}S_{ij} = 0.15 = 0.48 \max(2Q)$ in red. Green: isosurface of streamwise velocity $u = \min[u(x, y = 0, z)]$. (Box shifted by $12L_x/64$)

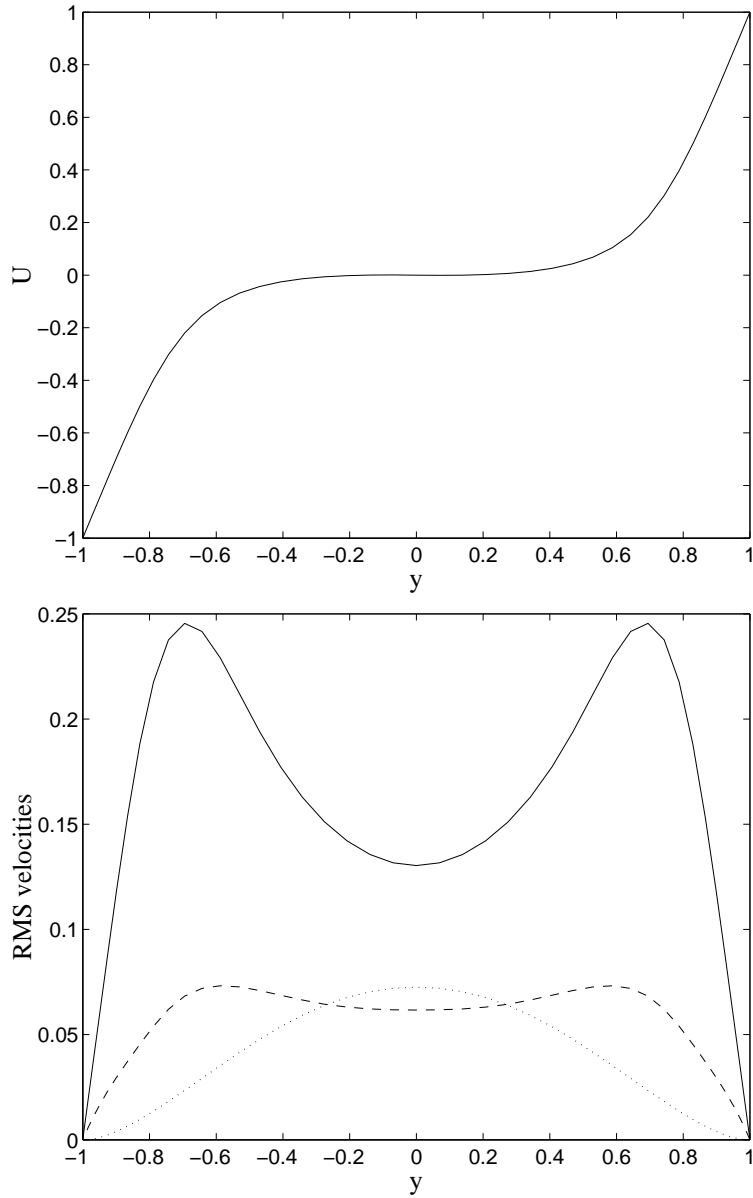


Figure 4: Mean and RMS velocity profiles for upper branch steady solution in no-slip plane Couette flow with $\alpha = 1.14$, $\gamma = 2.505$ and $R = 400$. Solid: u , dot: v , dash: w .

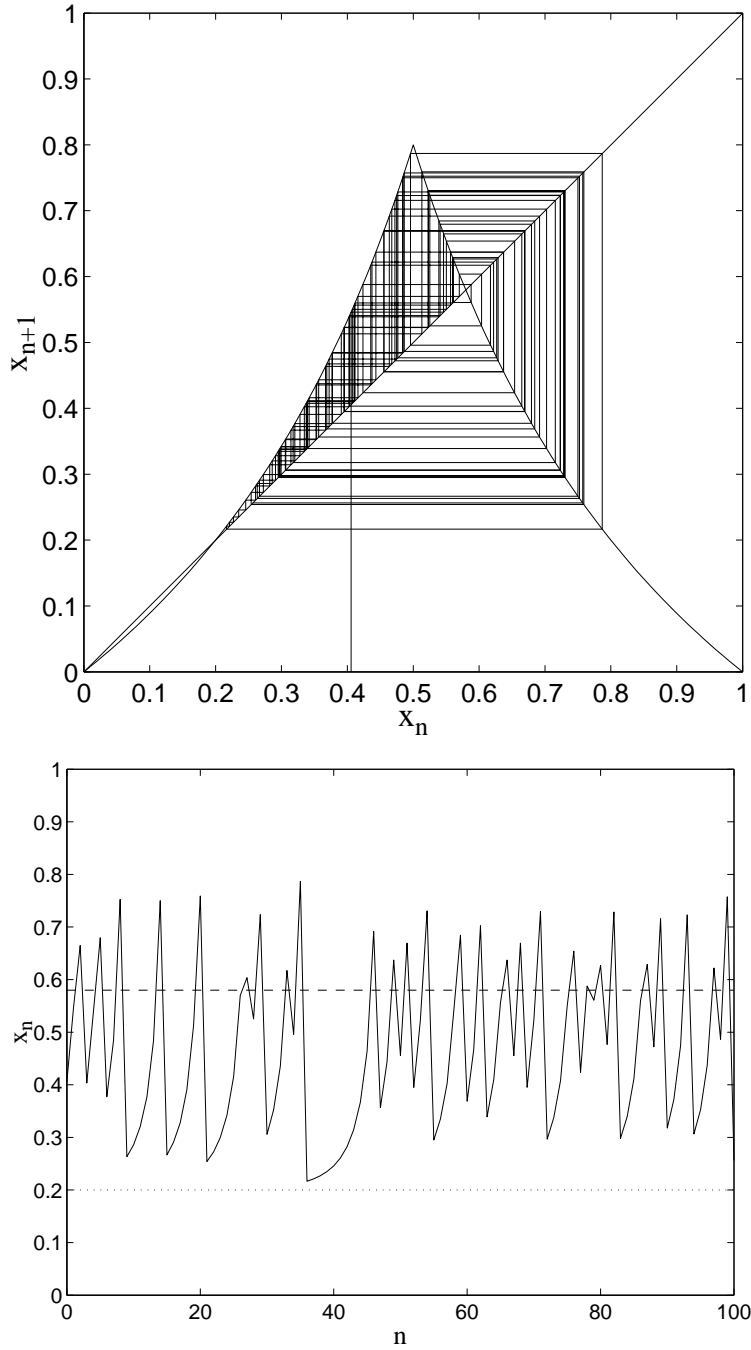


Figure 5: Top: the map $x_{n+1} = f_\mu(x_n)$ in (18) and 100 iterates from $x_0 \approx 0.4057$ and $\mu = 0.8$. Bottom: x_n vs. n for same μ and x_0 , dash is upper branch x_u , dot is lower branch x_l .

fixed points (or period 1 orbit) as well as an infinite number of periodic solutions. But all those new solutions are unstable from onset and remain so for all $R > R_c$. The lower branch is $x_\ell = 1 - \mu$. It is clear that all initial conditions in $1 - \mu < x_0 < \mu$ will be trapped in that interval forever, yet there are no stable fixed point or periodic solutions in that interval. The dynamics of that simple map is illustrated in fig. 5 for $\mu = 0.8$ and $x_0 = 4.057062130620955e - 01$ (picked randomly from a uniform distribution). The solution consists of a chaotic oscillation about the upper branch with excursions toward the lower branch and slow escape from that point, leading to intermittent behavior. Clearly, the upper branch solution $x_u = (\sqrt{\mu^2 + 4\mu} - \mu)/2$ provides a good first approximation to the average x_n in the chaotic regime. More precisely, it provides an upper bound on the average. The lower branch and its stable manifold are the separatrix, or the ‘basin boundary’ [7] that separates the basin of attraction of the stable trivial fixed point from the chaotic basin. The period two solution $x_1 = [\sqrt{(\mu + 1)^2 + 4} - (\mu + 1)] / 2$, $x_2 = f(x_1)$, would provide a next order approximation, etc.

This model is at present not connected with the Navier-Stokes equations. However it might be obtained from them in a manner similar to that of Lorenz [10] by plotting successive maxima of one variable against each other. The maxima of a variable such as W in sect. 3 above, that suitably measures the amplitude of the streak instability eigenmode, is a good candidate for that. In any case, the simple map (18) contains several of the key dynamical characteristics of shear flows: the existence of a simple fixed point stable for all Reynolds numbers, the onset of non-trivial but unstable fixed points and periodic orbits at a finite Reynolds number R_c and the apparently sudden transition to turbulence. Slight modifications of the model can also account for *strange repellors* [18] and for a sudden transition to chaos occurring after the onset of unstable states.

In this simple view, the turbulent flow is seen as an ‘oscillation’ about an upper branch or period-1 solution and the stable manifold of the lower branch is essentially the phase space boundary between the basin of attraction of the stable laminar state and the turbulent domain. This is roughly similar to the view of Toh and Itano [7] with the added information that the turbulence is an ‘oscillation’ about the upper branch solutions. Toh and Itano do not discuss the role of upper branch solutions, which are probably inaccessible to their shooting method. Toh and Itano view ‘bursting’ as the phase space motion along the unstable manifold of the lower branch solution. That is an example of how the inherent instabilities of the coherent structures could lead to explanations of further characteristics of turbulence.

Acknowledgements

The author is grateful for funding through grant NSF-DMS-0204636 and to Leslie Smith, Roger Waleffe and Derek Waleffe for allowing him to write this article on evenings and week-ends.

References

- [1] R.J. Adrian, C.D. Meinhart, C.D. Tomkins, Vortex organization in the outer region of the turbulent boundary layer, *J. Fluid Mech.*, **422**, 1-54 (2000).
- [2] R.M. Clever & F.H. Busse, Three-dimensional convection in a horizontal layer subjected to constant shear, *J. Fluid Mech.* **234**, 511–527 (1992),

- [3] O. Dauchot & N. Vioujard, Phase space analysis of a dynamical model for subcritical transition to turbulence in plane Couette flow, *Euro. Phys. J. B* **14**, 377-381 (2000).
- [4] R.M. Clever & F.H. Busse, Tertiary and quaternary solutions for plane Couette flow, *J. Fluid Mech.* **344**, 137–153 (1997).
- [5] P. Holmes, J.L. Lumley & G. Berkooz, *Turbulence, Coherent Structures, Dynamical Systems and Symmetry*, Cambridge University Press, Cambridge/New York, 1996.
- [6] J.M. Hamilton, J. Kim & F. Waleffe, Regeneration mechanisms of near-wall turbulence structures, *J. Fluid Mech.* **287**, 317–348 (1995).
- [7] T. Itano & S. Toh, The dynamics of bursting process in wall turbulence, *J. Phys. Soc. Japan*, **70**, 701–714 (2001).
- [8] J. Jimenez and P. Moin, The minimal flow unit in near-wall turbulence, *J. Fluid Mech.* **225**, 213-240 (1991).
- [9] G. Kawahara & S. Kida, Periodic motion embedded in plane Couette turbulence: regeneration cycle and burst, *J. Fluid Mech.* **449**, 291–300 (2001).
- [10] E.N. Lorenz, Deterministic Nonperiodic Flow, *J. Atmos. Sci.* **20**, 130–141 (1963).
- [11] M. Nagata, Three-dimensional finite-amplitude solutions in plane Couette flow: bifurcation from infinity, *J. Fluid Mech.* **217**, 519–527 (1990).
- [12] C.R. Smith & S.P. Metzler, The characteristics of low-speed streaks in the near-wall region of a turbulent boundary layer, *J. Fluid Mech.* **129**, pp. 27-54 (1983).
- [13] S. Toh & T. Itano, Low-dimensional dynamics embedded in a plane Poiseuille flow turbulence: Traveling-wave solution is a saddle point?, xxx.lanl.gov/abs/physics/9905012 (1999).
- [14] F. Waleffe, Hydrodynamic stability and turbulence: beyond transients to a self-sustaining process, *Stud. Appl. Math.* **95**, 319-343 (1995).
- [15] F. Waleffe, On a self-sustaining process in shear flows, *Phys. Fluids* **9**, 883–900 (1997).
- [16] F. Waleffe, Three-dimensional coherent states in plane shear flows, *Phys. Rev. Lett.* **81**, 4140–4143 (1998).
- [17] F. Waleffe, Exact coherent structures in channel flow, *J. Fluid Mech.* **435**, 93–102 (2001).
- [18] F. Waleffe, Homotopy of exact coherent structures in plane shear flows, submitted to *Phys. Fluids* (Aug. 13, 2002)